Available online at www.sciencedirect.com
ScienceDirect
Scripta Materialia 77 (2014) 56–59
Scripta MATERIALIA
www.elsevier.com/locate/scriptamat

Deformation and stress at pop-in of lithium niobate induced by nanoindentation

Zhenyu Zhang,[a,b,c,*] Song Yang,[a] Chaoge Xu,[a] Bo Wang[a] and Nengdong Duan[a]

[a] *Key Laboratory for Precision and Non-Traditional Machining Technology of Ministry of Education, Dalian University of Technology, Dalian 116024, People's Republic of China*
[b] *State Key Laboratory of Tribology, Tsinghua University, Beijing 100084, People's Republic of China*
[c] *State Key Laboratory of Metastable Materials Science and Technology, Yanshan University, Qinhuangdao 066004, People's Republic of China*

Received 6 January 2014; revised 20 January 2014; accepted 20 January 2014
Available online 26 January 2014

The hardness of X-, Y- and Z-cut lithium niobate ($LiNbO_3$ or LN) is 12.8, 9.1 and 10.6 GPa, respectively. The pop-in phenomenon was observed for all loading experimental data of nanoindentation, which was induced by the formation of twins, confirmed using sub-nanometer scale transmission electron microscopy. The maximum shear stresses at pop-in for X-, Y- and Z-cut LN wafers are 20.6, 13.3 and 18.4 GPa, respectively, and the corresponding stresses are 25.5, 21 and 20 GPa.

Keywords: Deformation; Maximum shear stress; TEM; Nanoindentation; Lithium niobate

Lithium niobate ($LiNbO_3$ or LN) is a wide-gap ferroelectric material with a unique combination of physical properties, including excellent electro-, acousto- and nonlinear optical characteristics [1–4]. It is also called the "silicon of photonics", and is indispensable in advanced photonics and nonlinear optics [1]. Thus, LN continues to be a workhouse material for critical applications in photonic devices [4]. This metal oxide is desirable due to its high electro-optic coefficient, as well as intrinsic insulating properties. These properties have made LN a standard material for applications in ultrahigh-speed modulators or for radiofrequency photonics [4].

Before it is suitable for use in a high-performance device, LN must undergo several machining processes, usually consisting of wiresaw slicing from an ingot, followed by grinding or lapping, mechanical polishing, and finally chemical mechanical polishing, to produce a qualified wafer that is free of both cracks and subsurface damage [5–7]. The surface roughness of a qualified wafer used in an LN device is less than 1 nm [8].

LN also has unique mechanical characteristics. For instance, the lattice constants of LN are 5.219 and 13.756 Å for the *a* and *c* axes [10], respectively, so the ratio of c/a is 2.64. It has been reported that, in a solid, a c/a ratio of >1.5 is characteristic of kinking nonlinear elastic solids [9]. Therefore, LN belongs to this unusual class. Furthermore, the hardness of LN is in a transition area between soft-brittle and hard-brittle solids. For example, both cadmium zinc telluride and mercury cadmium telluride are soft-brittle solids, and their hardness varied from 0.5 to 1.1 GPa [11–13]. Silicon is a hard-brittle solid, and has a hardness ranging from 12 to 14 GPa [11]. The Vickers microhardness of LN was determined to be 6.3 GPa under a 2 N load [14]. These mechanical properties give LN a brittle, tough and relatively soft (Mohs 5) nature [5,9,15]. Traditional lapping, grinding and mechanical polishing generated defects in machined LN specimens, such as scratches and free imbedded abrasives [5,16]. This shows that LN is a difficult-to-machine material. Nevertheless, ultrasmooth and damage-free wafers of LN are stringently required for use in high-performance photonic devices.

Fundamental mechanical deformation of LN is a prerequisite for the successful fabrication and operation of high-performance devices [9]. Despite its importance, few publications are available on such deformation [9,17]. In this work, we report our recent findings on

* Corresponding author at: Key Laboratory for Precision and Non-Traditional Machining Technology of Ministry of Education, Dalian University of Technology, Dalian 116024, People's Republic of China; e-mail: zzy@dlut.edu.cn

1359-6462/$ - see front matter
http://dx.doi.org/10.1016/j.scriptamat.2014.01.018

the mechanical deformation and stress at pop-in of LN wafers induced by nanoindentation.

LN wafers were obtained by slicing, lapping and chemical mechanical polishing. Our double-polished LN wafers were 50 mm in diameter and 1 mm in thickness. X-, Y- and Z-cut orientations were used as specimens for nanoindentation. The surface roughness was measured by use of a noncontact precision profilometer (Newview 5022, ZYGO, USA). The arithmetic surface roughness, R_a, of the X-, Y- and Z-cut samples was 0.51 ± 0.02, 0.99 ± 0.09 and 0.95 ± 0.31 nm, respectively, and the corresponding peak-to-valley was 13.9 ± 2.1, 9.2 ± 0.5 and 8.4 ± 2.0 nm. Nanoindentation was performed using a TriboIndenter® nanoindenter (Hysitron Inc., Minneapolis, MN). A Berkovich indenter, with a tip radius of 150 nm, calibrated on a standard quartz supported by Hysitron Inc., was employed to conduct the nanoindentation tests. The loading, dwelling and unloading times were kept constant at 10, 10 and 10 s, respectively. Peak loads were set at 1, 2, 3, 4, 5, 6, 8 and 10 mN for different tests. For each peak load, 10 repetitions were carried out at different locations spaced at intervals of 10 μm, except for the peak load of 10 mN. The residual indents after unloading were characterized by atomic force microscopy (AFM), using the microscope that was incorporated with the nanoindenter. To prepare cross-sectional transmission electron microscopy (TEM) specimens, nanoindentations at a peak load of 10 mN were conducted 100 times for each orientation of wafer at intervals of 20 μm. Cross-sectional TEM specimens were prepared using focused ion beam milling (Helios 600I, FEI, Netherlands), then thinned using a Gatan Model 691 precision ion polishing system, operated by an ion gun with low energy, varying from 0.5 to 2 keV, for 40 min. TEM characterizations were conducted using a sub-nanometer scale transmission electron microscope (JEOL JEM-ARM200F Cs corrected S/TEM).

Figure 1 shows typical load–displacement data of X-, Y- and Z-cuts of LN wafers at a peak load of 10 mN. The load–displacement data are illustrated by 5–10 curves incorporated for each orientation. This means that the nanoindentation measurements show good repeatability. Pop-ins are observed and AFM images show the pile-up phenomenon for all three orientations, indicating that plastic deformation occurred. This is consistent with previous reports on nanoindentation of LN [9,17]. Cracks are absent in the three AFM images. The sizes of the AFM images are approximately 2 μm. As the sizes of the nanoindentations are very small, we made a pattern mode of 100 indentations at a peak load of 10 mN for each orientation for this pattern to be shown up under a microscope.

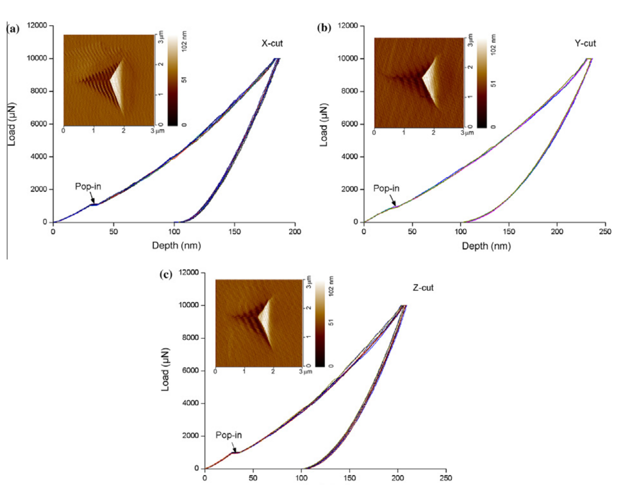

Figure 1. Load–displacement data of (a) X-cut, (b) Y-cut and (c) Z-cut LN wafers at a peak load of 10 mN. The insets show the corresponding AFM images of the residual impression after unloading.

Figure 2 shows the hardness and elastic modulus of the X-, Y- and Z-cut LN wafers as a function of load. An indentation size effect of hardness appears, which is in good agreement with previous reports [17]. The hardness of the X-, Y- and Z-cut LN wafers, shown in Figure 2(a), is around 12.8, 9.1 and 10.6 GPa, respectively, at peak loads varying from 4 to 10 mN, and the corresponding elastic modulus is about 209.6, 98.3 and 172.2 GPa (Figure 2(b)). This agrees well with previous presentations [17].

It is interesting that pop-in occurred for all the load–displacement data at about 1 mN (Figure 1). We postulate that elastic deformation occurred prior to pop-in, and that this started the plastic deformation. If this assumption is correct, the fundamental mechanism of deformation at pop-in of LN is extremely significant for the nanomanufacture of high-performance LN photonic devices. We thus investigated the fundamental deformation mechanism and stress at pop-in of LN wafers under specific loading conditions.

Figure 3 shows typical cross-sectional TEM images of Y-cut wafer at a peak load of 10 mN at both low and high magnifications. The inset in Figure 3(a) shows the corresponding selected area electron diffraction (SAED) pattern. Four pairs of regular double-dot patterns marked with black arrows are evident in the SAED pattern, indicating the formation of twins [18]. This is confirmed by Figure 3(b) and (c). Twins are formed along the (0 0 6) plane, and are symmetrical along the (0 1 2) plane. Hence, the mechanical deformation at pop-in shown in Figure 1 was formed by the formation of twins. This is attributed to the hexagonal lattice of LN with much smaller slip planes [19]. The X-, Y- and Z-cuts are represented by Miller indices of (1 1 0), (1 0 0) and (0 0 1), respectively. A conversion formula from the Miller to the Miller–Bravais index is

$$(hkl) \rightarrow (hk-(h+k)l) \qquad (1)$$

Using this conversion, the X-, Y- and Z-cuts correspond to (11 2 −0), (10 1 −0) and (0001) in

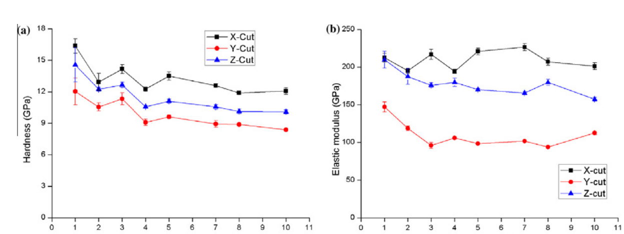

Figure 2. (a) Hardness and (b) elastic modulus of X-, Y- and Z-cut LN wafers as a function of load.